

Ab Initio Calculations of the ^{17}O NMR Chemical Shift of Hydronium and Dihydroxonium Ions in Their Fluoroborates: Comparison with Experiment

Dan Fărcașiu* and Dan Hâncu

Department of Chemical and Petroleum Engineering, University of Pittsburgh, 1249 Benedum Hall, Pittsburgh, Pennsylvania 15261

Received: July 22, 1998; In Final Form: October 12, 1998

The geometries of the hydronium and dihydroxonium cations in ion pairs with fluoroborate anions were examined by ab initio calculations at the MP2/6-31G* level. It was found that the representation of the hydronium ion in the field of an anion as an equilateral triangle, employed in the literature for the interpretation of low-temperature broad-band NMR spectra of water in solid acids, is an oversimplification, particularly for the composition H_5O_2^+ (dihydroxonium). Chemical shift calculations (DFT–GIAO–B3LYP at the dzvp, tzp, tz2p, and qz2p levels) were conducted for ^{17}O in $\text{H}_3\text{O}^+\cdot\text{BF}_4^-$ (**1**) and $\text{H}_5\text{O}_2^+\cdot\text{BF}_4^-$ (**2**). The signal of **2** was predicted to appear at higher frequency (downfield) than the signal for **1**. For experimental verification, the ^{17}O NMR spectra were recorded for various mixtures of hydronium fluoroborate and water. A nonmonotonic variation of the ^{17}O chemical shift with the increase in water content was observed; the signal moved first toward higher frequency and had the highest chemical shift for a water-to-hydronium ratio of 1:1 (H_5O_2^+), after which a monotonic variation toward lower frequency (upfield) was observed. Along both branches of the δ ^{17}O vs composition plot ($\text{H}_3\text{O}^+\cdot\text{BF}_4^-$ to $\text{H}_5\text{O}_2^+\cdot\text{BF}_4^-$ and $\text{H}_5\text{O}_2^+\cdot\text{BF}_4^-$ to H_2O) the chemical shift variation was nonlinear. Thus, the experiments and the calculations were in qualitative agreement (the signal for **1** at lower frequency than the signal for **2**), but the chemical shift difference predicted by the calculations was larger than the experimental result. Better agreement between the calculated and measured chemical shift differences is obtained for an orientation of ions in **2** with two fluorine atoms hydrogen bonded with the cation. Likewise, a better agreement is obtained for the pyramidal form than for the planar form of **1**, in agreement with the geometry optimization results.

Introduction

We reported recently on the effect of ion pairing on the structure of carbocations.¹ We have also studied the effect of ion pairing upon the properties of another type of cation, the hydronium ion.

In our studies of acid strength of liquid and solid acid catalysts, we have concentrated on two groups of probe bases suitable for investigation by NMR: alkenones² and aromatic hydrocarbons.^{2d,3} There are, however, quite a few studies in which water was used as probe base for acidity studies. In the early work, the acidity function of $\text{FSO}_3\text{H}-\text{SbF}_5$ (14–82 mol % SbF_5) was determined from the lifetime of dissolved hydronium ions, measured by dynamic NMR spectroscopy.⁴ The low sensitivity of the NMR method required the use of high concentrations of water (4–15 mol %),⁴ conditions under which the H_0 parameter does not measure the actual acid strength.^{2c,5} Indeed, determination of acidity functions by NMR is possible only for indicator concentrations extrapolated to infinite dilution.² Moreover, the whole treatment⁴ was based on the acidity of the hydronium ion (the $\text{p}K_{\text{BH}^+}$ value of water), a property found later to be highly variable.⁶ The reported acid strengths⁴ and basicity constants⁷ should, therefore, be very much in error.

More recently, an evaluation of relative acid strengths of various media, especially solids, was attempted from the extent of hydration of near-stoichiometric quantities of water. The methods used were (1) high-resolution ^1H MAS NMR spectroscopy at room temperature,⁸ (2) deconvolution of broad-band ^1H NMR spectra of frozen water at 4 K,⁹ (3) IR spectroscopy,¹⁰

(4) neutron diffraction,¹¹ and (5) pump–probe measurements by picosecond IR laser pulses.¹² Evaluations by theoretical calculations of the extent of hydration of water by molecules modeling the zeolites were also published.¹³ As pointed out earlier,⁶ these methods gave conflicting results.¹⁴

The controversy stimulated us to examine whether ^{17}O NMR spectroscopy¹⁵ could be applied to determine the level of hydration of water, just as ^{13}C NMR had been applied to the study of carbon bases.^{2,3} The very large natural width of ^{17}O lines is only partially narrowed by the pulse (FT) technique¹⁶ or by proton decoupling,¹⁷ but appropriate pulse sequences give accurate chemical shifts.¹⁸ The very wide range of ^{17}O chemical shifts¹⁹ could allow the signals of partially hydrated water to be distinguished from those of other oxygen-containing compounds in the mixture. The large second-order quadrupolar broadening of ^{17}O lines of solid samples²⁰ is reduced by dynamic angle spinning (DAS)^{20a} and double rotation (DOR).^{20b} Because on solids and in concentrated solutions the hydration gives ion pairs, we investigated computationally and experimentally the hydronium fluoroborate (**1**, $\text{H}_3\text{O}^+\cdot\text{BF}_4^-$) and the dihydroxonium fluoroborate (**2**, $\text{H}_5\text{O}_2^+\cdot\text{BF}_4^-$).

Methods

Theoretical Calculations. All calculations were conducted with the Gaussian 94 series of programs.²¹ The geometry optimizations were performed at the MP2/6-31G* level, whereas the chemical shifts were obtained from DFT–GIAO (gauge-including atomic orbitals) calculations at the B3LYP level.²²

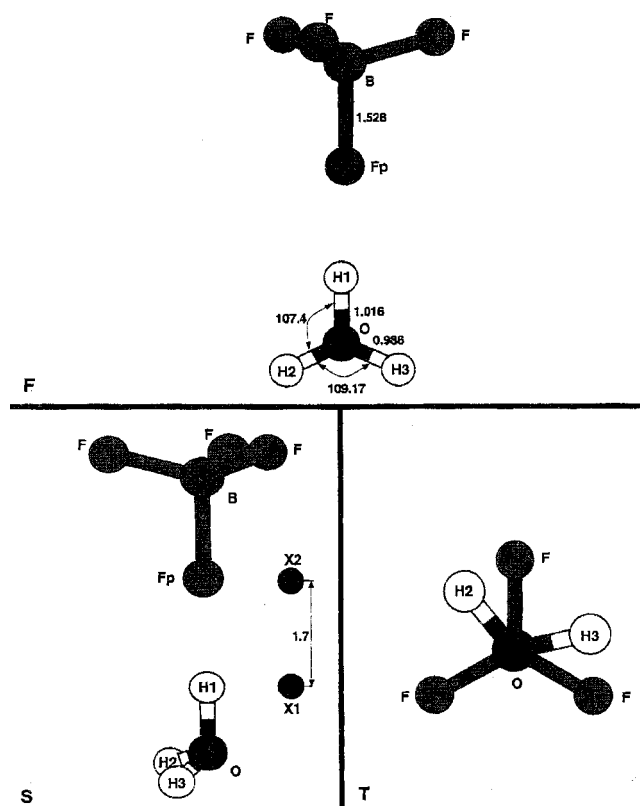
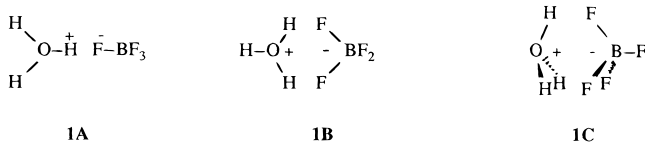


Figure 1. Optimized (MP2/6-31G*) geometry of the $\text{H}_3\text{O}^+\cdot\text{BF}_4^-$ ion pair in the orientation allowing one H-F hydrogen bond (**1A**). **F**: front view, X1, X2, dummy atoms. **S**: side view. **T**: top view, dummy atoms not represented.

The basis sets employed were^{1b} dzvp (9s5p1d/3s2p1d for B, O, F and 5s/2s for H),^{23a} tzp (9s5p1d/ 5s3p1d for B, O, F and 5s1p/3s1p for H),^{23b} tz2p (11s6p3d/5s3p2d for B, O, F and 5s3p/3s2p for H),^{23c} and qz2p (11s7p2d/6s4p2d for B, O, F and 6s2p/3s2p for H).^{23d}

As in our previous work, the relative orientation and the distance between the ions in the ion pair were controlled in the calculations through the use of “dummy” atoms.^{1,24} Three orientations of the hydronium fluoroborate, **1A**, **1B**, and **1C**, with one, two, and three hydrogen bonds between anion and cation were examined.



In orientation **1A** (Figure 1), two “dummy” atoms, X1 and X2, were used. The distance X1-X2, fixed, defined the interionic distance, d . In one series of calculations, the orientation was fixed; that is, the angles $\theta(\text{O}-\text{H}_1-\text{X}_1)$, $\theta(\text{H}_1-\text{X}_1-\text{X}_2)$, $\theta(\text{X}_1-\text{X}_2-\text{Fp})$, and $\theta(\text{X}_2-\text{Fp}-\text{B})$, where Fp is the fluorine closest to the cation (proximal fluorine atom), were held at 90° , whereas the dihedral angles $\varphi(\text{O}-\text{H}_1-\text{X}_1-\text{X}_2)$ and $\varphi(\text{X}_1-\text{X}_2-\text{Fp}-\text{B})$ were held at 180° . The variable parameters, $\varphi(\text{H}_1-\text{X}_1-\text{X}_2-\text{Fp})$ and $d(\text{X}_2-\text{Fp})$, allowed the anion to glide freely (plane-parallel movement), with Fp in a plane perpendicular to the O-H1 bond; the distance from this plane to H1 was equal to the fixed distance $d(\text{X}_1-\text{X}_2)$. The ion pair was first optimized with $\varphi(\text{H}_1-\text{O}-\text{H}_2-\text{H}_3) = 0^\circ$, that is, a planar cation. Then, starting with the optimized planar

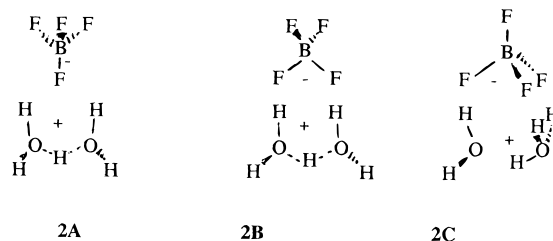
structure, $\varphi(\text{H}_1-\text{O}-\text{H}_2-\text{H}_3)$ was allowed to vary in order to obtain the nonplanar geometry of the cation in the ion pair **1**.

To optimize the relative orientation of the ions, in the next calculations only the angles $\theta(\text{O}-\text{X}_1-\text{X}_2) = \theta(\text{X}_1-\text{X}_2-\text{B}) = 90^\circ$ and the interionic distance X1-X2 (d) were frozen. All other parameters were optimized, with the initial values for $\varphi(\text{H}_1-\text{O}-\text{X}_1-\text{X}_2)$ and $\varphi(\text{X}_1-\text{X}_2-\text{B}-\text{Fp})$ being 0° .

In orientation **1B**, X1 was again “connected” to O at a fixed distance; X1-X2 = d and $\theta(\text{O}-\text{X}_1-\text{X}_2) = \theta(\text{X}_1-\text{X}_2-\text{B}) = 90^\circ$ were constant. The starting geometry had the adjacent BH_2 and OH_2 groups coplanar; that is, $\varphi(\text{F}_1-\text{B}-\text{X}_2-\text{X}_1) = \varphi(\text{F}_2-\text{B}-\text{X}_2-\text{X}_1) = \varphi(\text{X}_2-\text{X}_1-\text{O}-\text{H}_1) = \varphi(\text{X}_2-\text{X}_1-\text{O}-\text{H}_2) = 0^\circ$, then the parameters defining relative position of the ions, $d(\text{X}_2-\text{B})$, $\theta(\text{X}_2-\text{B}-\text{F})$, and $\varphi(\text{B}-\text{X}_2-\text{X}_1-\text{O})$ were optimized as were all the internal coordinates in the cation and anion.

In the third orientation, **1C**, three dummy atoms were employed to define the geometry (Figure 2): Two of them, X1 and X2, together with the oxygen defined a basal plane for the cation. The third, X3, was placed on a line X2-X3 perpendicular to the X1OX2 plane. The anion was positioned such that the angle $\theta(\text{X}_2-\text{X}_3-\text{B})$ was held at 90° . The anion glided over the cation, with B in a plane parallel to X1OX2, a movement controlled by the optimization of the X3-B distance and of the dihedral angle $\varphi(\text{O}-\text{X}_2-\text{X}_3-\text{B})$. The distance between the two planes was determined by the fixed distance X2-X3 (d). As in the previous cases of optimization of the relative position of the ions, the anion rotated freely around any axis passing through the boron atom.

The dihydroxonium ion pair (**2**) was also examined in three relative orientations of the ions. In the first orientation, **2A**, the description of the geometry used two dummy atoms, X1 and X2, such that X1-X2 was perpendicular to the O1O2X1 plane. X1 was placed on the line perpendicular to O1-O2 in the middle of the latter (Figure 3). The angles $\theta(\text{X}_1-\text{X}_2-\text{Fp}) = \theta(\text{X}_2-\text{Fp}-\text{B}) = 90^\circ$ and $\varphi(\text{X}_1-\text{X}_2-\text{Fp}-\text{B}) = 180^\circ$ were held constant. The anion moved such that the proximal fluorine glided in a plane parallel to the O1O2X1 plane; the distance between the two planes was $d(\text{X}_1-\text{X}_2)$.



In the other two orientations (**2B**, **2C**) of the ions in the ion pair **2**, three dummy atoms were employed (illustrated in Figure 4). The first, X1, was the same as in the previous case; the second, X2, was midway between O1 and O2 ($\text{O}_1-\text{X}_2 = \text{X}_2-\text{O}_2$, $\theta(\text{O}_1-\text{X}_2-\text{X}_1) = \theta(\text{O}_2-\text{X}_2-\text{X}_1) = 90^\circ$), and the third, X3, was such that X1-X3 was perpendicular to the O1O2X1 plane. The anion could move with the boron atom kept in a plane parallel to O1O2X1 at the fixed distance $d(\text{X}_1-\text{X}_3)$ by optimization of the distance X3-B and dihedral angle $\varphi(\text{X}_2-\text{X}_1-\text{X}_3-\text{B})$. The angle $\theta(\text{X}_1-\text{X}_3-\text{B}) = 90^\circ$ was constant. The anion was also allowed to rotate around any axis passing through the boron atom.

The projections of the molecular geometry shown here were generated with the computer program XMOL.²⁵

Experimental Determination of NMR Spectra. Hydronium tetrafluoroborate was prepared by absorbing BF_3 into a 1:1 mixture of hydrogen fluoride and water, with the materials,

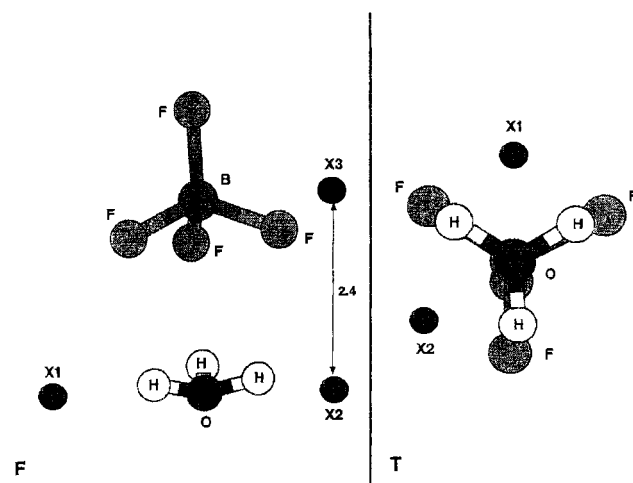


Figure 2. Partially optimized (MP2/6-31G*) geometry of the $\text{H}_3\text{O}^+\cdot\text{BF}_4^-$ ion pair in the orientation allowing three H–F hydrogen bonds, **1C** (immediately before decomposition to H_2O , HF, and BF_3). F and T as in Figure 1.

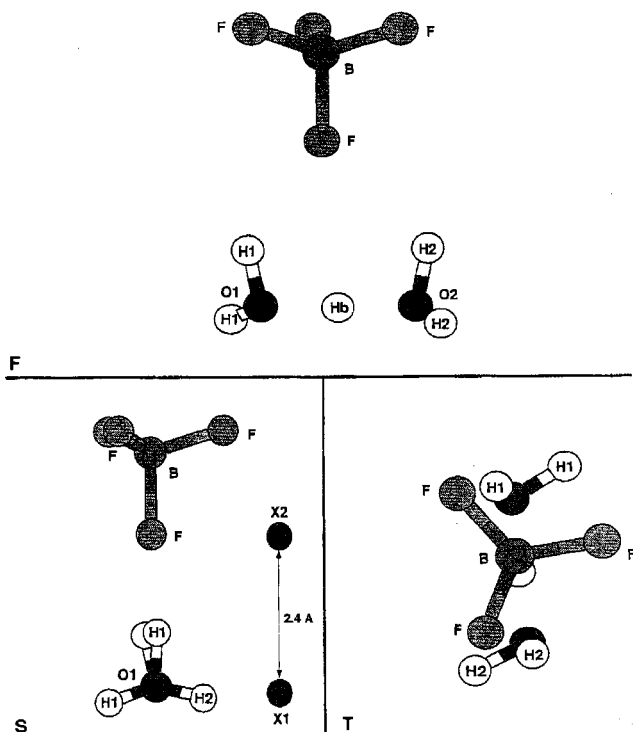


Figure 3. Partially optimized (MP2/6-31G*) geometry of the $\text{H}_5\text{O}_2^+\cdot\text{BF}_4^-$ ion pair in the orientation allowing one H–F hydrogen bond, **2A** (the bridging hydrogen, Hb, does not find an equilibrium position). F, S and T as in Figure 1.

installation, and procedure described in our previous paper.⁶ The solid product (mp 38 °C) was kept in a Kel-F tube, in a desiccator with P_2O_5 . Its concentration was determined both by titration with NaOH in the presence of CaCl_2 and by placing its melting point on the calibration curve for hydronium fluoroborate–water mixtures, as described before.⁶ The more dilute mixtures were prepared by adding the appropriate amounts of water to the most concentrated solution, determining the weight with an analytical balance.

All spectra were recorded on a Bruker DMX 300 instrument at the base frequency of 40.6882 MHz for ^{17}O . The samples were prepared in 8 mm NMR tubes placed coaxially in standard, thin-walled, 10 mm NMR tubes containing distilled water as the chemical shift standard. It was important to cap tightly the

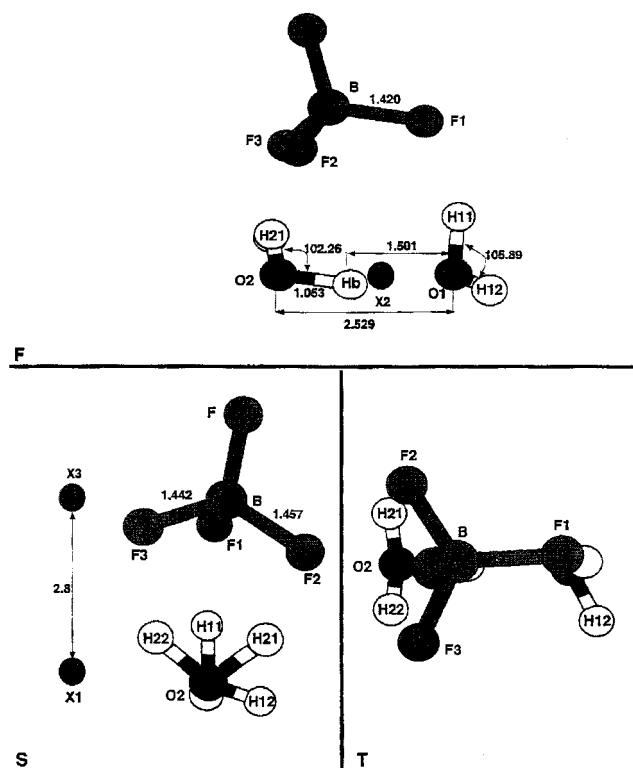


Figure 4. Optimized (MP2/6-31G*) geometry of the $\text{H}_5\text{O}_2^+\cdot\text{BF}_4^-$ ion pair at the interionic distance of 2.8 Å (the preferred orientation allows three H–F hydrogen bonds, **2C**). F, S and T as in Figure 1.

8 mm tubes, otherwise the signal for the most concentrated sample would drift because of absorption of moisture. All the spectra were run at 40 °C, just above the melting point of the highest melting sample. A sequence consisting of an excitation pulse of 8 μs followed by a recovery delay of 30 ms before acquisition and a relaxation delay of 1 s was employed, with proton decoupling by a Waltz sequence. A total of 6000 transients were accumulated for each spectrum.

Results and Discussion

Theoretical Evaluation of Structures and Chemical Shifts.

Ab initio calculations of NMR chemical shifts have been used to choose among possible structures or conformations of carbocations.²⁶ Valid predictions were made for structures that were not energy minima but had one^{26b,c} or two negative frequencies^{26a} in the force constant matrixes. In one case, a conformation resulting from the geometry optimization as a transition state was accepted as the true structure because the calculated chemical shift for its sp^2 carbon was the closest to experiment.^{26c}

Various properties of hydronium ion and its clusters with water molecules have been examined by ab initio calculations.²⁷ Chemical shift calculations on the isolated cations by the IGLO method²² gave a larger (higher frequency) chemical shift for H_5O_2^+ than for H_3O^+ .^{27b} We have seen before that ^{13}C shifts calculated for structures optimized in ion pairs are closer to experiment than the values obtained for isolated carbocation structures.^{1b} We decided to check whether calculations on **1** and **2** would agree with the experimental values, which we also set out to measure.

The ^{17}O NMR spectrum of hydronium ion was first recorded in superacid solution.²⁸ The nondecoupled signal, a quartet, indicated the absence of exchange at that acid strength. It was noted that the hydration shift (less than 10 ppm toward higher

TABLE 1: Geometrical Parameters for $\text{H}_3\text{O}^+\cdot\text{BF}_4^-$ (1A**)^a at MP2/6-31G***

parameter	value	
	planar cation ^b	pyramidal cation
$d(\text{O}-\text{H}1)$	0.980	1.016
$d(\text{O}-\text{H}2)$	0.972	0.986
$d(\text{O}-\text{H}3)$	0.972	0.986
$d(\text{B}-\text{Fp})$	1.476	1.528
$\theta(\text{H}1-\text{O}-\text{H}2)$	119.52	107.40
$\theta(\text{H}2-\text{O}-\text{H}3)$	120.97	109.17
$\varphi(\text{H}1-\text{O}-\text{H}2-\text{H}3)$	180.00 ^c	116.45
charge at H1	0.49	0.59
charge at H2, H3	0.46	0.56

^a Closest interionic distance, $d(\text{H}1-\text{Fp}) = 1.7 \text{ \AA}$. ^b Forced geometry, higher in energy than the pyramidal geometry by 4.22 kcal/mol. ^c Kept constant during the optimization.

frequency) is small compared to the large hydration shifts observed in carbon spectra of organic bases. The oxygen resonances of carbonyl compounds shift, however, toward lower frequency (upfield) by about 250 ppm upon hydration, which means that the chemical shift is controlled by the change in the extent of π bonding at oxygen and the positive charge has only a minor effect.²⁹ The spectrum of the hydronium ion was first rationalized as proving a planar geometry for the cation,²⁸ but theoretical calculations on the isolated ion indicated a pyramidal structure.³⁰

Information about ions **1** and **2** in ion pairs was provided by a ^1H NMR study in which the counterion was the complex of octanesulfonic acid with SbCl_5 and the solvent was a mixture of Freons.³¹ The spectrum of **1** consisted of a doublet (2H), δ 11.1 ppm, and a triplet (1H), δ 8.3 ppm, indicating either one or two hydrogen bonds within the ion pair.³¹ The author favored a structure of the type **1B** on the assumption that hydrogen bonding should be deshielding. A planar structure was preferred for H_3O^+ because the coupling constant, 2.8 Hz, was smaller than the value reported for water, 7.2 Hz.³² It was also argued that a pyramidal cation should favor the orientation **1C**.³¹

We began, therefore, with the optimization of **1A** with the cation held planar. The distance between the cation and anion, d (defined in the Methods) was fixed at 1.7 \AA . The final structure was reoptimized without a planarity restriction and led to the pyramidal geometry. This result confirms the calculations on the isolated ion³⁰ but contradicts the conclusion based on the ^1H NMR spectrum.³¹ It follows that the decrease in the coupling constant does not require that the oxygen hybridization changes to sp^2 . In fact, considering the higher electronegativity of oxygen in hydronium than in water, the variation in coupling constant upon the change in hybridization should follow the pattern of change from $\text{H}_a-\text{CH}_2-\text{H}_b$, $|J| = 12-15$, to $\text{H}_a-\text{C}(=\text{O})-\text{H}_b$, $|J| = 42$, rather than from $\text{H}_a-\text{CH}_2-\text{H}_b$ to $\text{H}_a-\text{C}(=\text{C}^-)-\text{H}_b$, $|J| = 2-3$.³³ The main geometrical parameters for both forms are listed in Table 1, and the more stable pyramidal geometry is shown in three projections in Figure 1. It can be noted that the equilibrium structure had O, H1, Fp, and B collinear.

When the anion was allowed to rotate (around any axis passing through B) at $X1-X2 = 4.23 \text{ \AA}$ (initial $\text{H}1-\text{Fp} = 1.7 \text{ \AA}$), the ion pair decomposed to BF_3 , HF, and water. Moving the anion farther away, to an initial $\text{H}1-\text{Fp}$ distance of 2.2 \AA ($X1-X2 = 4.73 \text{ \AA}$), did not change this outcome.

The relative orientations of the anion and cation in the ion pair with two (**1B**) and three anion-cation hydrogen bonds (**1C**) were also examined, as described in the Methods. For each orientation, the anion was allowed to glide freely in a plane placed above the cation ($X1-X2 = 2.4 \text{ \AA}$). The calculations

were started with the planar cation. In each case, optimization resulted in a minor tilting movement of the anion and pyramidalization of the cation, followed by decomposition to H_2O , HF, and BF_3 . Because the closest H-F distance in **1B** (1.53 \AA) was shorter than that in **1A** (above) and **1C** (1.7 \AA), optimization of **1B** was also conducted at a longer interionic distance ($X1-X2 = 3.2 \text{ \AA}$, initial $\text{H}1-\text{Fp} = 2.2 \text{ \AA}$), with the same result. The geometry of the ion pair in orientations **1C** just before the decomposition is shown in Figure 2.

For the dihydroxonium ion, the reported ^1H NMR spectrum in an ion pair at low temperature (94 K) consisted of two singlets of intensity ratio 1:4 (δ 21.3 and 6.0 ppm, respectively).³¹ This result indicates that the anion is found somewhere in the space between the two oxygen atoms of the complex cation. Therefore, we considered in calculations only relative orientations satisfying this condition. Again, three possibilities were examined, with one (**2A**), two (**2B**), and three fluorine atoms of the anion facing the cation (**2C**), as defined in the Methods.

In orientation **2A**, the proximal fluorine atom (Fp) was allowed to glide in a plane parallel to the axis connecting the oxygen atoms. The B-Fp bond was held perpendicular to that plane. The ion pair adopted after optimization the structure of Figure 3, in which one hydrogen at each oxygen faces the anion and the cation is close to the C_2 symmetry predicted for the isolated species.^{27b,34} The bridging proton, Hb, did not find an equilibrium position but continued to shift around the midpoint of the O1-O2 distance, with insignificant variations in energy, after the rest of the system did not change any more from one optimization cycle to the next. This orientation was 4 kcal/mol less stable than the alternative discussed below.

Orientation **2B** was optimized with the anion free to rotate around any axis passing through the boron atom, which was allowed to glide in a plane parallel to the O1-O2 axis of the cation, at 2.8 \AA from it. This distance was chosen to give an H-F distance close to 1.7 \AA , appropriate for the length of a hydrogen bond. The system reoriented itself into the third orientation, **2C**. In this arrangement, one hydrogen bonded to O1 and two hydrogens bonded to O2 are turned toward the anion, each toward a fluorine atom. Significantly, the bridging hydrogen (Hb) is not equidistant from the two oxygen atoms, but it is bonded to O2 ($d = 1.053 \text{ \AA}$) and hydrogen bonded to O1 ($d = 1.501 \text{ \AA}$). The angle $\theta(\text{O}1-\text{Hb}-\text{O}2)$ is 163.7°. For comparison, the isolated cation had $d(\text{O}1-\text{Hb}) = d(\text{O}2-\text{Hb}) = 1.193 \text{ \AA}$ and $\theta(\text{O}1-\text{Hb}-\text{O}2) = 174.6^\circ$.^{27b} The optimized structure of **2C** is shown in Figure 4, and its main geometrical parameters are given in Table 2. The nonsymmetrical placement of Hb between O1 and O2 might reflect the unequal interaction of the anion with the two water molecules bridged by Hb. Because both H21 and H22 face negative fluorine atoms in the anion, there is a higher electron density at O2 than at O1 and O2 can more strongly coordinate the hydron Hb.

When the distance between the plane that contains the boron atom and the O1-O2 axis was increased to 3.3 \AA , optimization of **2C** led to an orientation **2B**, in which the anion is tilted such that one of the B-F bonds is essentially in the plane in which the boron atom can move (Figure 5.) The main geometrical parameters are also listed in Table 2.

The results of the calculation have to be interpreted in light of the results of the ^1H NMR study.³¹ The observation of one signal for all the "outer" hydrogens (H11, H12, H21, and H22 in Figures 4 and 5) requires a conformational mobility in the ion pair at 94 K. An inversion of configuration in **2C** (chiral) requires the rotation of the water molecules around O1-O2, rotation of the anion, and the shift of Hb from O2 to O1, which

TABLE 2: Geometrical Parameters for $\text{H}_3\text{O}_2^+\cdot\text{BF}_4^-$ (2**) at MP2/6-31G***

parameter	value	
	2C ^a	2B ^b
$d(\text{O1}-\text{O2})$	2.529	2.528
$d(\text{O1}-\text{H11})$	0.990	0.989
$d(\text{O1}-\text{H12})$	0.972	0.972
$d(\text{H}_b-\text{O2})$	1.053	1.047
$d(\text{H}_b-\text{O1})$	1.501	1.498
$d(\text{H21}-\text{O2})$	1.017	1.106
$d(\text{H22}-\text{O2})$	1.007	0.977
$d(\text{B}-\text{F1})$	1.420	1.427
$d(\text{B}-\text{F2})$	1.457	1.538
$d(\text{B}-\text{F3})$	1.442	1.375
$\theta(\text{O1}-\text{H}_b-\text{O2})$	163.68	166.63
$\theta(\text{H11}-\text{O1}-\text{H12})$	105.89	105.55
$\theta(\text{H21}-\text{O2}-\text{H}_b)$	102.26	103.78
$\theta(\text{H21}-\text{O2}-\text{H22})$	96.47	107.27
$\varphi(\text{H21}-\text{O2}-\text{H22}-\text{H}_b)$	104.17	111.17
$\varphi(\text{H21}-\text{O2}-\text{O1}-\text{H11})$	-48.99	-16.52
$\varphi(\text{B}-\text{X3}-\text{X1}-\text{X2})$	-11.38	-14.87
$\varphi(\text{F1}-\text{B}-\text{X3}-\text{X1})$	79.85	64.44
$\varphi(\text{F2}-\text{B}-\text{X3}-\text{X1})$	-20.0	-66.76
$\varphi(\text{F3}-\text{B}-\text{X3}-\text{X1})$	-65.56	-89.95

^a Interionic distance (between boron and the O1–O2 axis) is 2.8 Å (Figure 4). ^b Interionic distance is 3.3 Å (Figure 5).

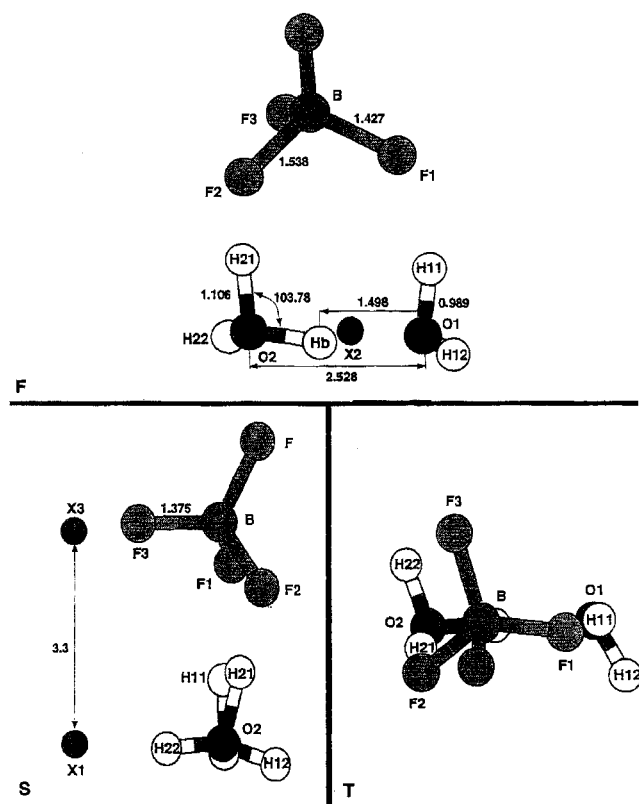


Figure 5. Optimized (MP2/6-31G*) geometry of the $\text{H}_3\text{O}_2^+\cdot\text{BF}_4^-$ ion pair at the interionic distance of 3.3 Å (the preferred orientation allows two H–F hydrogen bonds, **2B**). **F**, **S** and **T** as in Figure 1.

explains the observed absence of spin–spin coupling.³¹ An interconversion of **2C** and **2B** is possible. It was not tested, however, (for instance by osmometry) whether isolated ion pairs or clusters of four ions ($\text{A}^-\cdot\text{C}^+\cdot\text{A}^-\cdot\text{C}^+$) or larger were present in the Freon solution.³¹ Therefore, caution against overinterpreting the experimental spectra is in order.

None of the optimized structures are true energy minima for the ion pairs, because release of all constraints led to decomposition to HF, BF_3 , and water. The interaction between ion

pairs in larger aggregates seems necessary for the stability of hydronium fluoroborate. Nonetheless, the optimized structures of the cations in **1** and **2** are satisfactory descriptions of the respective cations in the field of the fluoroborate anion. Indeed, examination of the *tert*-butyl cation in a five-ion aggregate $\text{Li}^+\cdot\text{H}_3\text{BF}^-\cdot\text{Me}_3\text{C}^+\cdot\text{FBH}_3^-\cdot\text{Li}^+$, which does not undergo ion recombination, and in the triple ion $\text{H}_3\text{BF}^-\cdot\text{Me}_3\text{C}^+\cdot\text{FBH}_3^-$, which does, showed that geometry optimization at fixed interionic distances gives reliable structures for carbocations in ion pairs or aggregates.²⁴

The results of our calculations, together with the ^1H NMR spectra,³¹ are relevant for the interpretation of broad-band ^1H NMR spectra at 4 K.⁹ The dihydroxonium ion was considered there as a noninteracting mixture of a hydronium ion and a molecule of water.⁹ Instead, it is possible that the proton shift from O1 and O2 is more like a vibration and is still occurring at 4 K. As a matter of fact, both H21H22Hb and, especially, H11H12Hb are scalene triangles, rather than equilateral and isosceles, respectively, as assumed.⁹ Even the hydronium ion in a single ion pair has unequal O–H bonds and is, therefore, not an equilateral triangle. The distortions in the latter case might, however, be too small for the accuracy of the broad-band NMR method.

As shown in a previous study, the structures optimized for cations in ion pairs are appropriate for NMR chemical shift calculations.^{1b} The energy of **2B** is higher than that of **2C**, but the greater interionic distance in the latter makes this result a preordained conclusion. We calculated, therefore, the ^{17}O isotropic shield constants by the DFT–GIAO–B3LYP method for both **2B** (at 3.3 Å) and **2C** (at 2.8 Å) and for the pyramidal and planar forms of **1A**. Whereas the GIAO–MP2 method is in principle superior and the chemical shifts calculated with it give better agreement with the measured values,³⁵ GIAO–B3LYP calculations have been found successful in some applications.^{1b} Use of larger basis sets may compensate to some extent for the deficiencies of the DFT calculations. The comparison with the experimental results that we obtained may help to evaluate the usefulness of the DFT chemical shift calculations. Because finding energy differences was not our goal, we did not apply a correction for basis set superposition error.³⁶

The absolute chemical shifts for all species and the relative chemical shift of **1** and **2** are shown in Table 3. The calculations predict the correct ordering of chemical shifts, **1** at a lower frequency than **2**, but the chemical shift difference calculated is larger than the expected uncertainty of the method.³⁵ Increasing the basis set from dzvp to tzp improves the chemical shift difference, and upon further increase to tz2p and qz2p, shielding constant values appear to converge. The difference $\delta(\mathbf{2}) - \delta(\mathbf{1})$ is still greater than the experimental value. A better fit might be perhaps secured by slight changes of the interionic distances, but this would be an arbitrary move as long as experimental data on the actual interionic distances in **1** and **2** are not available. Better agreement is obtained for orientation **2C** than for **2B** and likewise for the pyramidal than for the planar form of **1A**, the latter being in line with the geometry optimization results.

^{17}O Spectra of Hydronium Fluoroborate–Water Mixtures. The use of chemical shifts for determination of degrees of hydration is based on linear interpolation between the signals for the base and its conjugate acid. For a calibration of chemical shifts with the degree of conversion of water to hydronium ions, a potential uncertainty is introduced by the incomplete ionization of the acid (source of hydrons). Therefore,

TABLE 3: Calculated Isotropic Shielding Constants (σ) and Chemical Shifts (δ) for 1A and 2B^a

basis set	isotropic shielding constant (σ) ^b									$\Delta\delta(2-1A)$ ^c			
	$\text{H}_3\text{O}^+\cdot\text{BF}_4^-$ (1A)		$\text{H}_5\text{O}_2^+\cdot\text{BF}_4^-$ (2B)			$\text{H}_5\text{O}_2^+\cdot\text{BF}_4^-$ (2C)			2B-1A		2C-1A		
	planar	pyramidal	O1	O2	avg	O1	O2	avg	<i>d</i>	<i>e</i>	<i>d</i>	<i>e</i>	
dzvp ^f	305	290	261	282	271.5	247	281	264	33.5	18.5	41	26	
tzp ^g	305	292	275	302	288.5	258	302	280	16.5	3.5	25	12	
tz2p ^h	299	296	267	287	277	252	286	269	22	19	30	27	
qz2p ⁱ	299	291	265	287	276	251	286	268	23	15	31	23	
expr										~5 ^j		~5 ^j	

^a By the DFT-GIAO-B3LYP method, on optimized (MP2/6-31G*) structures. ^b In ppm. ^c $\Delta\delta(2-1) = (\sigma_{\text{ref}} - \sigma_2) - (\sigma_{\text{ref}} - \sigma_1) = \sigma_1 - \sigma_2$. ^d Planar H_3O^+ . ^e Pyramidal H_3O^+ . ^f From ref 23a. ^g From ref 23b. ^h Polarization exponents (contraction coefficients) are 1.0414 (0.357851), 0.3085 (0.759561), 0.295 (1.00) for B and 2.82 (0.357851), 0.83 (0.759561), 0.67 (1.00) for O (J. Gauss, ref 23c); the other values are as in ref 1b. ⁱ Polarization exponents are 0.29 and 0.87 for B, 2.08 and 0.69 for O (J. Gauss, ref 23d); the other values are as in ref 1b. ^j Difference (11.5-6.5), cf. Figure 7.

TABLE 4: ^{17}O Chemical Shifts of Hydronium Fluoroborate-Water Mixtures at 38 °C

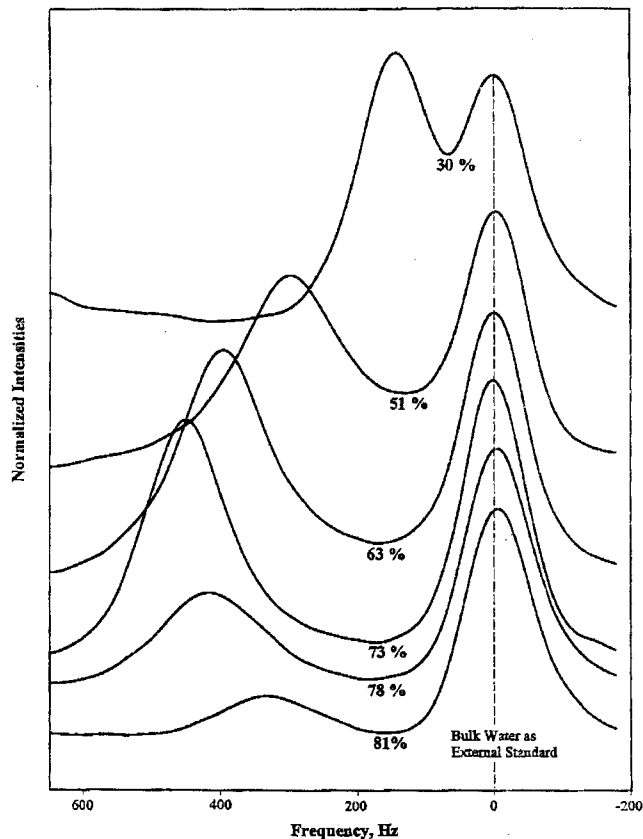
% HBF ₄	mol % H ₂ O ^a	H ₂ O/H ₃ O ⁺ (mol/mol)	δ ^{17}O (ppm) ^b
0	100	∞	0
30.3	91.1	10.221	3.0
51.2	78.5	3.649	7.5
63.2	64.8	1.840	9.7
72.9	44.9	0.813	11.1
77.7	28.6	0.400	10.34
80.75 ^c	14.0	0.163	8.3

^a The balance to 100% consists of H_3O^+ . ^b Water used as external standard. ^c Pure hydronium fluoroborate is 82.6% HBF₄.

the calibration must be based on the water solutions of a "nonexisting acid," such as chloroaluminic³⁷ and fluoroboric,³⁸ which is present in solution entirely as the hydronium salt. We investigated the hydronium fluoroborate,³⁹ obtained as described in a previous paper,⁶ in the presence of increasing amounts of water. The spectra were run at 40 °C, the lowest temperature at which the most concentrated sample was still liquid.

As shown in Table 4, the chemical shift variation between water and hydronium fluoroborate is nonmonotonic. Starting from the most concentrated solutions, the averaged ^{17}O signal moves first toward higher frequency (downfield) and then toward lower frequency (upfield). This variation is also shown by the spectra plotted in Figure 6 for 30–81% HBF₄ solutions. The signal of the external standard, water, is also shown in each spectrum. Therefore, the degree of hydronation of water cannot be determined by ^{17}O NMR spectroscopy because for most of the range between 0% and 100% hydronation any chemical shift corresponds to two compositions. As shown in Figure 7, the largest chemical shift corresponds to $\text{H}_5\text{O}_2^+\cdot\text{BF}_4^-$, which means that dihydroxonium fluoroborate (2) behaves like a compound rather than as a mixture, which should show chemical shift additivity. Moreover, the chemical shift variation along each of the two branches of the curve (from $\text{H}_3\text{O}^+\cdot\text{BF}_4^-$ to $\text{H}_5\text{O}_2^+\cdot\text{BF}_4^-$ and from $\text{H}_5\text{O}_2^+\cdot\text{BF}_4^-$ to H_2O) is nonlinear. As the viscosity increases, the line width of the signal for the $\text{H}_3\text{O}^+\cdot x\text{H}_2\text{O}$ aggregate also increases for the most concentrated solutions.

The variation of ^{17}O chemical shifts with the concentration of hydronium ions in water was studied before only in the dilute acid range.⁴⁰ By extrapolation of values obtained for molar fractions of acids between 0 and about 0.16, a chemical shift of 66.8 ± 1.1 ppm was calculated for H_3O^+ ,^{40b} in total disagreement with the values determined for this species in superacid,²⁸ as well as with our measurements. (We note that extrapolation of the chemical shift change measured by us between 0% and 8.9% H_3O^+ in water gives a "predicted" value

**Figure 6.** ^{17}O NMR spectra of fluoroboric acid solutions ($\text{H}_3\text{O}^+\cdot x\text{H}_2\text{O}\cdot\text{BF}_4^-$).

of more than 30 ppm for the hydronium ion, also in complete disagreement with the experimental value.)

A study of dilute solutions of various salts of the ammonium cation, considered not to affect water chemical shifts,⁴¹ was used to establish that there is a significant effect of anions upon the chemical shifts of water.⁴⁰ A correction for the anion effect cannot remove, however, the large discrepancies mentioned above. We note that the two values reported from direct measurements in superacid^{28,29} and our data were obtained with different anions and in different media, yet they are in reasonable agreement, giving an average value of 9 ± 2.5 ppm for the ^{17}O chemical shift of the hydronium ion. Moreover, it was found that the acid anions produce a shift of the water signal toward higher frequency,⁴⁰ meaning that the discrepancy (66.8 ± 1.1 vs 9 ± 2.5 ppm) is in the wrong direction. Also, the anion effect cannot explain the maximum observed by us in the variation of chemical shift with the $\text{H}_3\text{O}^+/\text{H}_2\text{O}$ ratio (Figure 7). The discrepancy is thus rather a proof of the dangers of extrapolation,

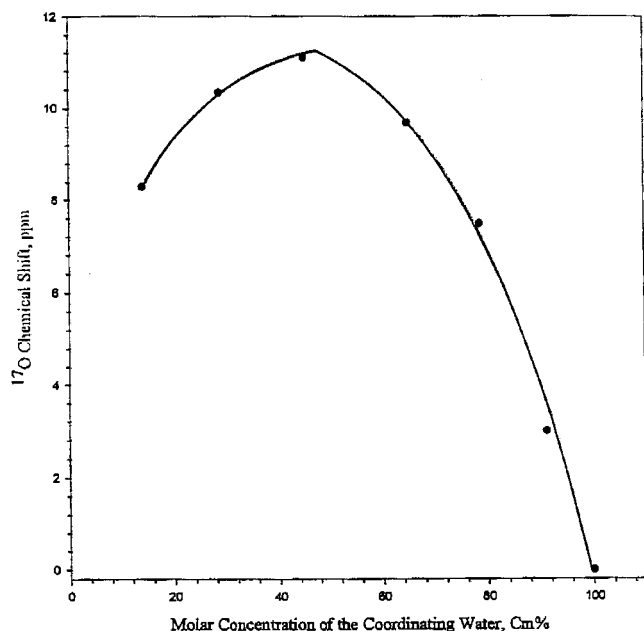


Figure 7. Variation of ^{17}O chemical shift of $\text{H}_3\text{O}^+\cdot x\text{H}_2\text{O}$ with composition (value of x).

particularly important in the case of a correlation involving the molecules of water and its conjugate acid and base.

Conclusions

The pattern of variation of the ^{17}O chemical shift in the system $\text{BF}_4^-\cdot\text{H}_3\text{O}^+\cdot x\text{H}_2\text{O}$ with the increase in water content (x), showing a maximum for $x = 1$, suggests that dihydroxonium ion (H_5O_2^+) is a compound rather than a mixture, which should show chemical shift additivity. The ab initio chemical shift calculations by the DFT—GIAO—B3LYP method conducted on $\text{H}_3\text{O}^+\cdot\text{BF}_4^-$ and $\text{H}_5\text{O}_2^+\cdot\text{BF}_4^-$ ion pairs at the dzvp, tzp, tz2p, and qz2p levels were in qualitative agreement with the experiment (the signal for $\text{H}_3\text{O}^+\cdot\text{BF}_4^-$ at lower frequency than the signal for $\text{H}_5\text{O}_2^+\cdot\text{BF}_4^-$), but the chemical shift difference predicted by the calculations is larger than the experimental value. The agreement is better for the orientation of the dihydroxonium fluoroborate ion pair in which two fluorine atoms face the cation and establish hydrogen bonds with it (**2B**). Likewise, the pyramidal form of the hydronium ion gives a better agreement with the experiment, which is in line with the results of geometry optimization. Optimization of interionic distances for a perfect fit is not warranted, however, as long as the actual arrangement of the ion pairs in larger aggregates is not known.¹ On the other hand, the representation of the hydronium ion in the field of an anion as an equilateral triangle, employed in the literature for the interpretation of broad-band NMR spectra of water in solid acids at low temperature, is an oversimplification, particularly for the composition H_5O_2^+ (dihydroxonium).

Acknowledgment. This work was supported by a grant (CTS-9528412) from the NSF and by a grant, also from the NSF (CTS-9413698), for the purchase of the DMX300 NMR instrument. A number of grants of supercomputer time were obtained from the Pittsburgh Supercomputing Center. We are indebted to Prof. Kenneth D. Jordan and Dr. Carlos Gonzales for many helpful discussions and to Dr. James. R. Cheeseman, Prof. Jürgen Gauss, and Prof. Reinhart Ahlrichs for consultations on the basis sets.

References and Notes

- (1) (a) Fărcașiu, D.; Hâncu, D. *J. Phys. Chem.* **1997**, *101*, 8695. (b) Fărcașiu, D.; Hâncu, D.; Haw, J. F. *J. Phys. Chem.* **1998**, *102*, 2493.
- (2) (a) Fărcașiu, D.; Ghenciu, A.; Miller, G. J. *Catal.* **1992**, *134*, 118. (b) Fărcașiu, D.; Ghenciu, A. *J. Am. Chem. Soc.* **1993**, *115*, 10901. (c) Fărcașiu, D.; Ghenciu, A. *Prog. NMR Spectrosc.* **1996**, *29*, 129 and references therein. (d) Fărcașiu, D.; Ghenciu, A.; Marino, G.; Kastrup, R. V. *J. Mol. Catal., A* **1997**, *126*, 141.
- (3) (a) Fărcașiu, D.; Fisk, S. L.; Melchior, M. T.; Rose, K. D. *J. Org. Chem.* **1982**, *47*, 453. (b) Fărcașiu, D. *Acc. Chem. Res.* **1982**, *15*, 46. (c) Fărcașiu, D.; Marino, G.; Miller, G.; Kastrup, R. V. *J. Am. Chem. Soc.* **1989**, *111*, 7210. (d) Fărcașiu, D.; Ghenciu, A.; Marino, G.; Rose, K. D. *J. Am. Chem. Soc.* **1997**, *119*, 11826.
- (4) (a) Gold, V.; Laali, K.; Morris, K. P.; Zdunek, L. Z. *J. Chem. Soc. Chem. Commun.* **1981**, 770. (b) Gold, V.; Laali, K.; Morris, K. P.; Zdunek, L. Z. *J. Chem. Soc., Perkins Trans. 2* **1985**, 859.
- (5) (a) Hammett, L. P.; Deyrup, A. J. *J. Am. Chem. Soc.* **1932**, *54*, 2721. (b) Hammett, L. P. *Physical Organic Chemistry*; McGraw-Hill: New York, 1940; p 171ff. (c) Rochester, C. H. *Acidity Functions*; Organic Chemistry Monographs 17; Blomquist, A. T., Ed.; Academic Press: New York, 1970.
- (6) Fărcașiu, D.; Hâncu, D. *J. Chem. Soc., Faraday Trans.* **1997**, *93*, 2161.
- (7) Gold, V.; Laali, K.; Morris, K. P.; Zdunek, L. Z. *J. Chem. Soc., Perkins Trans. 2* **1985**, 865.
- (8) Hunger, M.; Freude, D.; Pfeifer, H. *J. Chem. Soc., Faraday Trans.* **1991**, *87*, 657.
- (9) (a) Batamack, P.; Dorémieux-Morin, C.; Fraissard, J.; Freude, D. *J. Phys. Chem.* **1991**, *95*, 3790. (b) Heeribout, L.; Semmer, V.; Batamack, P.; Dorémieux-Morin, C.; Vincent, R.; Fraissard, J. *Stud. Surf. Sci. Catal.* **1996**, *101*, 831. (c) For the method, see: Dorémieux-Morin, C. *J. Magn. Reson.* **1976**, *21*, 419 and subsequent papers.
- (10) (a) Zecchina, A.; Buzzoni, R.; Bordiga, S.; Geobaldo, F.; Scarano, D.; Ricchiardi, G.; Spoto, G. *Stud. Surf. Sci. Catal.* **1995**, *97*, 213. (b) Wakabayashi, F.; Kondo, J. N.; Domen, K.; Hirose, C. *J. Phys. Chem.*, **1996**, *100*, 1442. (c) Zecchina, A.; Geobaldo, F.; Spoto, G.; Bordiga, S.; Ricchiardi, G.; Buzzoni, R.; Petrini, G. *J. Phys. Chem.* **1996**, *100*, 16584.
- (11) Smith, L.; Cheetham, A. K.; Morris, R. E.; Marchese, L.; Thomas, J. M.; Wright, P. A.; Chen, J. *Science* **1996**, *271*, 799.
- (12) (a) Domen, K. (Tokyo Inst. of Technology), at the meeting of ref 15. (b) Fujino, T.; Kashitani, M.; Kano, S. S.; Wakabayashi, F.; Goto, F.; Ishida, M.; Wada, A.; Domen, K.; Hirose, C. Paper in preparation.
- (13) (a) Haase, F.; Sauer, J. *J. Am. Chem. Soc.* **1995**, *117*, 3780. (b) Krossner, M.; Sauer, J. *J. Phys. Chem.* **1996**, *100*, 6199. (c) Sauer, J. *Science* **1996**, *271*, 774. (d) van Santen, R.; Kramer, G. J. *Chem. Rev.* **1995**, *95*, 637. (e) Zygumunt, S. A.; Curtiss, L. A.; Iton, L. E.; Erhardt, M. K. *J. Phys. Chem.* **1996**, *100*, 6663.
- (14) Discussions in Catalytic Chemistry. I. Catalysis by Strong Solid Acids (Post-congress workshop, The 11th International Congress on Catalysis), Baltimore, MD, 6–7 July, 1996.
- (15) (a) Alder, F.; Yu, F. C. *Phys. Rev.* **1951**, *81*, 1967. (b) The early work was reviewed in the following: Silver, B. L.; Luz, Z. *Quart. Revs.* **1967**, *21*, 458.
- (16) (a) Dahn, H.; Schlunke, H. P.; Tömler, J. *Helv. Chim. Acta.* **1972**, *55*, 907. (b) Mateescu, G. D.; Wilson, L. A. 14th Experimental NMR Conference; Boulder, CO, 1973.
- (17) Earl, W. L.; Niederberger, W. *J. Magn. Reson.* **1977**, *27*, 351.
- (18) Canet, D.; Goulon-Ginet, C.; Marchal, A. P. *J. Magn. Reson.* **1976**, *22*, 537.
- (19) (a) Christ, H. A. *Helv. Phys. Acta (C. R. Soc. Suisse Phys.)* **1960**, *33*, 572. (b) Sohár, P. *Nuclear Magnetic Resonance Spectroscopy*; CRC Press: Boca Raton, FL, 1983; Vol. 2, p 260.
- (20) (a) Mueller, K. T.; Sun, B. Q.; Chingas, G. C.; Zwanziger, J. W.; Terao, T.; Pines, A. *J. Magn. Reson.* **1990**, *86*, 470. (b) Wu, Y.; Sun, B. Q.; Pines, A.; Samoson, A.; Lippmaa, E. *J. Magn. Reson.* **1990**, *89*, 297 and references therein.
- (21) Frisch, M. J.; Trucks, G. W.; Schlegel, H. B.; Gill, P. M. W.; Johnson, B. G.; Robb, M. A.; Cheeseman, J. R.; Keith, T.; Petersson, G. A.; Montgomery, J. A.; Raghavachari, K.; Al-Laham, M. A.; Zakrzewski, V. G.; Ortiz, J. V.; Foresman, J. B.; Cioslowski, J.; Stefanov, B. B.; Nanayakkara, A.; Challacombe, M.; Peng, C. Y.; Ayala, P. Y.; Chen, W.; Wong, M. W.; Andres, J. L.; Replogle, E. S.; Gomperts, R.; Martin, R. L.; Fox, D. J.; Binkley, J. S.; DeFrees, D. J.; Baker, J.; Stewart, J. P.; Head-Gordon, M.; Gonzalez, C.; Pople, J. A. *Gaussian 94*, revision D.3; Gaussian, Inc.: Pittsburgh, PA, 1995.
- (22) (a) Kutzelnigg, W.; Fleischer, U.; Schindler, M. In *NMR, Basic Principles and Progress*; Diehl, P.; Fluck, E.; Günther, H.; Kosfeld, R., Seelig, J., Eds.; Springer: Berlin, 1991; p 165. (b) Ditchfield, R. *Mol. Phys.* **1974**, *27*, 789. (c) Wolinski, K.; Hilton, J. F.; Pulay, P. *J. Am. Chem. Soc.* **1990**, *112*, 8251.
- (23) (a) Godbout, N.; Salahub, D. R.; Andzelm, J.; Wimmer, E. *Can. J. Chem.* **1992**, *70*, 560. (b) Schäfer, A.; Hüber, C.; Ahlrichs, R. *J. Chem.*

Phys. **1994**, *100*, 5829 (available from the web site ftp://ftp.chemie.uni-karlsruhe.de/pub/basis). (c) Dunning, T. H., Jr. *J. Chem. Phys.* **1970**, *53*, 2823. With polarization exponents from: Gauss, J. Personal communication. (d) Schäfer, A.; Horn, H.; Ahlrichs, R. *J. Chem. Phys.* **1991**, *97*, 2571 (available from the web site in ref 23b). With polarization exponents for B from: Gauss, J. Personal communication.

(24) Fărcașiu, D.; Lukinskas, P. *J. Phys. Chem.* **1998**, *102*, 10436.

(25) *Xmol*, version 1.3.1; Minnesota Supercomputing Center, Inc.: Minneapolis, MN, 1993.

(26) (a) Schleyer, P. v. R.; Koch, W.; Liu, B.; Fleischer, U. *J. Chem. Soc., Chem. Commun.* **1989**, 1098. (b) Schleyer, P. v. R.; Carneiro, J. W. de M.; Koch, W.; Forsyth, D. A. *J. Am. Chem. Soc.* **1991**, *113*, 3990. (c) Sieber, S.; Buzek, P.; Schleyer, P. v. R.; Koch, W.; Carneiro, J. W. de M. *J. Am. Chem. Soc.* **1993**, *115*, 259. (d) Sieber, S.; Schleyer, P. v. R.; Gauss, J. *J. Am. Chem. Soc.* **1993**, *115*, 6987.

(27) For example, see: (a) Mijoule, C.; Latajka, Z.; Borgis, D. *Chem. Phys. Lett.* **1993**, *208*, 264. (b) Janoscsek, R. *J. Mol. Struct.* **1994**, *321*, 45. (c) Wei, D.; Salahub, D. R. *J. Chem. Phys.* **1994**, *101*, 7633 and references therein. (d) Tuckerman, M.; Laasonen, K.; Sprik, M.; Parrinello, M. *J. Phys. Chem.* **1995**, *99*, 5749.

(28) Mateescu, G. D.; Benedikt, G. M. *J. Am. Chem. Soc.* **1979**, *101*, 3959.

(29) Olah, G. A.; Berrier, A. L.; Prakash, G. K. S. *J. Am. Chem. Soc.* **1982**, *104*, 2373.

(30) Rodwell, W. R.; Radom, L. *J. Am. Chem. Soc.* **1981**, *103*, 2865.

(31) Golubyev, N. S. *Khim. Fiz.* **1984**, *3*, 772.

(32) Holmes, J. R.; Kivelson, D.; Drinkard, W. C. *J. Chem. Phys.* **1962**, *37*, 150.

(33) Becker, E. D. *High-Resolution NMR. Theory and Applications*, 2nd ed.; Academic Press: New York, 1980; pp 95–96.

(34) (a) Del Bene, J. *J. Phys. Chem.* **1988**, *92*, 2874. (b) Del Bene, J.; Shavitt, I. *Int. J. Quantum Chem. Symp.* **1989**, *23*, 445.

(35) (a) Cheeseman, J. R.; Trucks, G. W.; Keith, T. A.; Frisch, M. J. *J. Phys. Chem.* **1996**, *104*, 5497 and erratum. (b) de Dios, A. C. *Prog. Nucl. Magn. Reson. Spectrosc.* **1996**, *29*, 229.

(36) Chalasinski, G.; Gutowski, M. *Chem. Rev.* **1988**, *88*, 943.

(37) Brown, H. C.; Pearsall, H. *J. Am. Chem. Soc.* **1951**, *73*, 4081.

(38) Pawlenko, S. Z. *Anorg. Allg. Chem.* **1965**, *334*, 292.

(39) Pawlenko, S. Z. *Anorg. Allg. Chem.* **1962**, *315*, 291.

(40) (a) Mäemets, V.; Koppel, I. *J. Chem. Soc., Faraday Trans.* **1996**, *92*, 3533. (b) Mäemets, V.; Koppel, I. *J. Chem. Soc., Faraday Trans.* **1997**, *93*, 1539.

(41) (a) Hindman, J. C. *J. Chem. Phys.* **1962**, *36*, 1000. (b) Luz, Z.; Yagil, G.; *J. Phys. Chem.*, **1966**, *70*, 554. (c) Fister, F.; Hertz, H. G. *Ber. Bunsen Ges. Phys. Chem.* **1967**, *71*, 1032.